

Article

## Dual-site Fluorescent Probe for Visualizing the Metabolism of Cys in Living Cells

Yongkang Yue, Fangjun Huo, Peng Ning, Yongbin Zhang, Jianbin Chao, Xiangming Meng, and Caixia Yin

*J. Am. Chem. Soc.*, **Just Accepted Manuscript** • DOI: 10.1021/jacs.6b12845 • Publication Date (Web): 07 Feb 2017

Downloaded from <http://pubs.acs.org> on February 7, 2017

### Just Accepted

“Just Accepted” manuscripts have been peer-reviewed and accepted for publication. They are posted online prior to technical editing, formatting for publication and author proofing. The American Chemical Society provides “Just Accepted” as a free service to the research community to expedite the dissemination of scientific material as soon as possible after acceptance. “Just Accepted” manuscripts appear in full in PDF format accompanied by an HTML abstract. “Just Accepted” manuscripts have been fully peer reviewed, but should not be considered the official version of record. They are accessible to all readers and citable by the Digital Object Identifier (DOI®). “Just Accepted” is an optional service offered to authors. Therefore, the “Just Accepted” Web site may not include all articles that will be published in the journal. After a manuscript is technically edited and formatted, it will be removed from the “Just Accepted” Web site and published as an ASAP article. Note that technical editing may introduce minor changes to the manuscript text and/or graphics which could affect content, and all legal disclaimers and ethical guidelines that apply to the journal pertain. ACS cannot be held responsible for errors or consequences arising from the use of information contained in these “Just Accepted” manuscripts.

# Dual-site Fluorescent Probe for Visualizing the Metabolism of Cys in Living Cells

Yongkang Yue,<sup>†,§</sup> Fangjun Huo,<sup>‡,§</sup> Peng Ning,<sup>¶</sup> Yongbin zhang,<sup>‡</sup> Jianbin Chao,<sup>‡</sup> Xiangming Meng,<sup>¶,\*</sup> Caixia Yin<sup>†,\*</sup>

<sup>†</sup>Key Laboratory of Chemical Biology and Molecular Engineering of Ministry of Education, Key Laboratory of Materials for Energy Conversion and Storage of Shanxi Province, Institute of Molecular Science, Shanxi University, Taiyuan 030006, China

<sup>‡</sup>Research Institute of Applied Chemistry, Shanxi University, Taiyuan 030006, China

<sup>¶</sup>Department of Chemistry, Anhui University, Hefei, 230601, China.

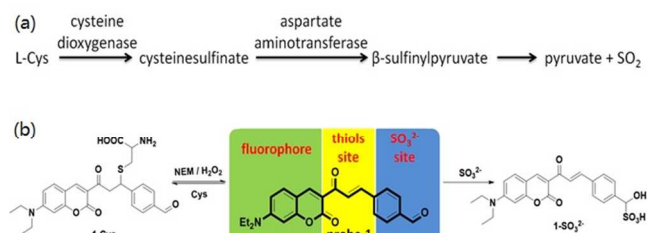
**ABSTRACT:** Fluorescent probes as non-invasive tools to visualize the metabolism of bio-molecules hold great potential to explore their physiological and pathological processes. For cysteine (Cys), however, none of the reported fluorescent probes could image the metabolic processes in living cells. To achieve this goal, we developed a coumarin derivate based on the rational design of the dual recognition sites for Cys and its metabolite SO<sub>2</sub>, respectively. The probe displayed distinct two channels turn-on fluorescent emission towards Cys and SO<sub>2</sub>, which were successfully applied for both A549 cells and zebra fish imagings. Further, with reversible fluorescent responses towards Cys, the probe could image the enzymatic conversion of Cys to SO<sub>2</sub> in living A549 cells though ratiometric manner. The present work reported the first probe to image the endogenous generated SO<sub>2</sub> without incubation of the SO<sub>2</sub> donors.

## INTRODUCTION

Cysteine (Cys) is one of the sulfhydryl contained small molecular amino acids playing crucial roles in many physiological and pathological processes. In biological systems, Cys can be generated primarily from methionine by methionineadenosyltransferase, adenosylhomocysteinase, cystathionine- $\beta$ -synthase, and cystathionine- $\gamma$ -lyase. Further for the consumption of Cys, the cysteine dioxygenase which existed in almost all of the mammals cells except erythrocyte catalyzes cysteine to cysteinesulfinate, and further converts to  $\beta$ -sulfinylpyruvate enzymatically by aspartate aminotransferase, then decomposes to pyruvate and SO<sub>2</sub>, which existed as the equilibrium of HSO<sub>3</sub><sup>-</sup> and SO<sub>3</sub><sup>2-</sup> in biological environments, spontaneously.<sup>1</sup> Normal level of Cys (30-200  $\mu$ M) maintains the synthesis of various proteins and the main antioxidant glutathione (GSH), and acted as the source of sulfide in human metabolism.<sup>2</sup> Excess amount of Cys, however, is associated with diseases including rheumatoid arthritis, Parkinson's disease, Alzheimer's disease.<sup>3</sup> At the same time, the deficiency of Cys was reported to cause slowed growth, edema, liver damage, skin lesions, and weakness.<sup>4</sup> Thus, to visualize the metabolism of the endogenous homeostasis of Cys is critical importance. Surely, many existed thiol fluorescent probes have been broadly used, such as determining Cys concentration from serum, or proteins, and cell imaging, replenish intracellular cysteine. However, to our knowledge, none of them realized the monitoring of the metabolism processes of Cys which were essential to gain deeper insight into the physiological and pathological roles of Cys.<sup>5</sup>

In this respect, fluorescent probes to visualize the metabolism processes of Cys should meet at least three prerequisites: a) the reaction between the probe and Cys should be reversible,<sup>6</sup> b) the fluorescent responses of probe towards the metabo-

lite (such as SO<sub>2</sub>) of Cys should be distinct with the probe-Cys system, c) both of the reaction processes should be fast to promote the real-time imaging. With these criteria in mind, we select  $\alpha,\beta$ -unsaturated ethanoylcoumarin as the fluorophore and the thiols reaction site which may feature reversible responses towards thiols with the addition of N-ethylmaleimide (NEM), a thiols scavenge reagent.<sup>7</sup> Besides, coumarin dyes were widely used in designing low toxicity fluorescent probes with excellent fluorescent properties which would benefit their biological applications.<sup>1e, 8</sup> Further, benzaldehyde moiety was one of the sensitive reaction site for SO<sub>2</sub> through nucleophilic addition reaction.<sup>8e, 9</sup> Combining ethanoylcoumarin with terephthalaldehyde, we develop **1** (Scheme 1 and Scheme S1) as the designed fluorescent probe to visualize metabolism of Cys in living cells. As expected, the dual site probe **1** can discriminatively detect thiols and sulfite through two emission channels with fast responses. Cell and zebra fish imaging experiments demonstrated the application of **1** serving as an appealing bioimaging probe. Further, as far as we know, **1** is the first reported probe to image the endogenous generated sulfur dioxide derivatives without incubation of the SO<sub>2</sub> donors such as Na<sub>2</sub>S<sub>2</sub>O<sub>3</sub> and 2,4-dinitrobenzene sulfonamide.<sup>1e, 10</sup>



**Scheme 1. (a) The aerobic metabolism process of Cys in mammal cells. (b) Designing of the dual-site fluorescent probe for Cys metabolism visualizing.**

## RESULTS AND DISCUSSION

**Fluorescent Responses of Probe 1 to Cys.** The UV-Vis and fluorescent responses of **1** towards Cys were firstly measured systematically upon addition of Cys with a gradually additive concentration range of 0 ~ 400  $\mu\text{M}$  to **1** in PBS-DMSO (1/1, v/v, pH 7.4) system. As shown in Figure 1a, **1** displayed non-fluorescent emission in the above system, however, the addition of Cys induced a turn-on fluorescent emission at 514 nm and peaked with a 130-fold enhancement. Accompanied with the fluorescent changes, the maximum absorption peak on UV-vis spectra changed from 475 nm to 450 nm (Figure S1). Time-dependent fluorescent response (Figure 1b) of **1** towards Cys (1 eq probe **1**: 20 eq Cys) at 514 nm displayed that the detection process balanced within 100 s and the subsequent fluorescent data were all measured 2 min after the addition of analyte. The corresponding detection limit based on the definition by IUPAC ( $\text{CDL} = 3 \text{ Sb/m}$ ) was 0.46  $\mu\text{M}$  from 10 blank solutions (Figure 1c). Notably, the fluorescent emission of Cys added **1** containing system could effectively be quenched by the addition of NEM which could be re-lighted by further addition of Cys (Figure 1d). The reversible cycling determinations: namely, five times supplement of Cys and subsequent NEM were carried out with negligible intensity attenuation which promoted **1** might be used as an efficient tool to real-time value the Cys concentrations in vitro and in vivo.

To value the effect of various analytes including amino acids, intracellular nucleophiles and  $\text{H}_2\text{O}_2$  towards probe **1**, 400  $\mu\text{M}$  Ala, Asn, Arg, Asp, Gln, Glu, Gly, His, Ile, Leu, Lys, Met, Phe, Pro, Ser, Thr, Trp, Tyr, Val,  $\text{SH}^-$ ,  $\text{SO}_3^{2-}$  and  $\text{H}_2\text{O}_2$  were added to **1** containing PBS-DMSO (1/1, v/v, pH 7.4) system, each. None of them could induce distinct fluorescent enhancement at 514 nm ( $\lambda_{\text{ex}} = 463 \text{ nm}$ ) (Figure S2). For the sulfydryl contained amino acids, 400  $\mu\text{M}$  Hcy induced almost the same fluorescent responses with 400  $\mu\text{M}$  Cys (Figure S3). Considering the physiological level of homocysteine (5-13  $\mu\text{M}$ ), the interference induced by homocysteine was negligible in the detection system.<sup>6, 11</sup> Besides, the reaction of probe with 1 mM GSH was hyperslow. Thus, probe **1** could detect Cys with relatively high selectivity. Further, the pH effect was measured upon addition of 400  $\mu\text{M}$  Cys into 20  $\mu\text{M}$  **1** in a mixture of DMSO/PB (1/1, v/v) with pH change from 3 to 12 (Figure S4). The spectra displayed that all there was strong emission at 514 nm with a 463 nm excitation in the range of pH 5~11. The obtained result showed detection process could realized in broad pH range.

Supported by the inert property of probe **1** towards  $\text{H}_2\text{O}_2$ , we wondered whether the fluorescence of Cys-probe **1** system could be quenched by the addition of  $\text{H}_2\text{O}_2$ , which could consume Cys to form cystine.<sup>12</sup> As shown in Figure S5,  $\text{H}_2\text{O}_2$  addition into probe **1**-Cys balanced system in PBS-DMSO (1/1, v/v, pH 7.4) induced distinct fluorescent intensity decrease and eventually quenched within 12 min at 514 nm. Upon the addition of Cys to the above quenched system, the fluorescent recovered dramatically (Figure S6). Considering the antioxidant nature of Cys, probe **1** might be used to monitor the redox dynamic in cells.

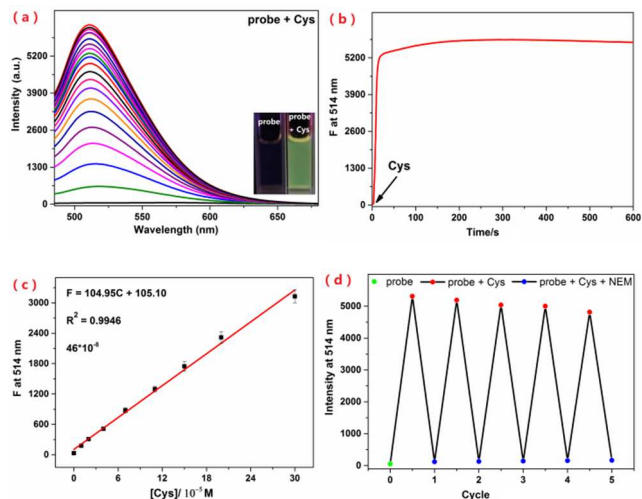


**Figure 1.** a) Fluorescent response of 20  $\mu\text{M}$  probe **1** upon addition of 400  $\mu\text{M}$  Cys in PBS/DMSO (1/1, v/v, pH 7.4) system. Insert: the corresponding fluorescent color change under the irradiation of a hand-held UV lamp. b) Time-dependent fluorescent emission of the 20  $\mu\text{M}$  probe **1** and 400  $\mu\text{M}$  Cys system at 514 nm. c) Working curve of **1** to detect Cys obtained by addition of various concentrations of Cys (0-300  $\mu\text{M}$ ) to 20  $\mu\text{M}$  probe **1**. d) Reversibility study of **1** (20  $\mu\text{M}$ ) towards Cys (400  $\mu\text{M}$ ) upon addition of NEM (400  $\mu\text{M}$ ).  $\lambda_{\text{ex}} = 463 \text{ nm}$ , slit: 5 nm/5 nm.

**Fluorescent Responses of Probe 1 to  $\text{SO}_3^{2-}$ .** For the sulfite detection, as we designed, the addition of  $\text{Na}_2\text{SO}_3$  into **1** containing PBS-DMSO (1/1, v/v, pH 7.4) system induced significant fluorescent emission centered at 576 nm with the excitation at 510 nm and peaked with 4-fold enhancement (Figure 2a). Similar to the above mentioned Cys detection system, the detection process of probe **1** towards  $\text{Na}_2\text{SO}_3$  (1 eq probe **1**: 20 eq  $\text{Na}_2\text{SO}_3$ ) balanced within 50 s which supported the following fluorescent data to be measured 1 min after the addition of analyte (Figure 2b). The detection limit of **1** towards  $\text{Na}_2\text{SO}_3$  was calculated to be 6.5  $\mu\text{M}$  (Figure 2c). Other analytes including various amino acids, especially for Cys, Hcy and GSH, and biological anions did not interfere the sulfite detection in above condition (Figure 2d). Besides, pH ranging from 4 to 8 was suitable for the detection process (Figure S8). These properties promoted **1** to discriminative detect thiols and sulfite through two emission channels.

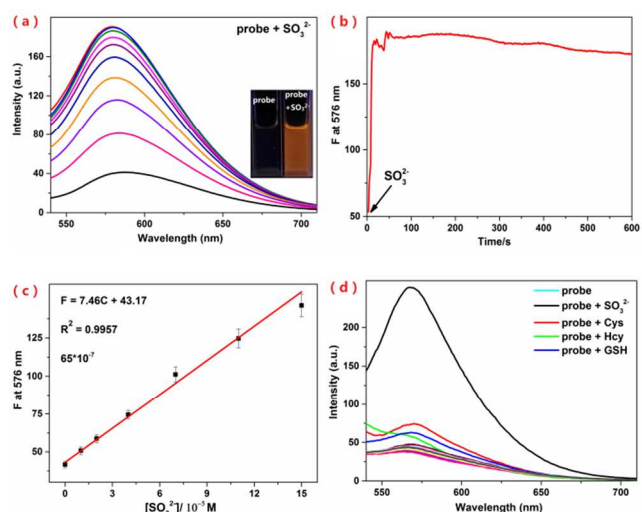


**Figure 2.** a) Fluorescent response of 20  $\mu\text{M}$  probe **1** upon addition of 400  $\mu\text{M}$   $\text{Na}_2\text{SO}_3$  in PBS/DMSO (1/1, v/v, pH 7.4) system. Insert: the corresponding fluorescent color change under the irradiation of a hand-held UV lamp. b) Time-dependent fluorescent emission of the 20  $\mu\text{M}$  probe **1** and 400  $\mu\text{M}$   $\text{Na}_2\text{SO}_3$  system at 576 nm. c) Working curve of **1** to detect  $\text{Na}_2\text{SO}_3$  obtained by addition of various concentrations of  $\text{Na}_2\text{SO}_3$  (0-150  $\mu\text{M}$ ) to 20  $\mu\text{M}$  probe **1**. d) Fluorescent responses of probe **1** towards 400  $\mu\text{M}$  Cys, Hcy, GSH, Ala, Asn, Arg, Asp, Gln, Glu, His, Lys, Met, Ser, Trp, Tyr,  $\text{SH}^-$ ,  $\text{F}^-$ ,  $\text{Cl}^-$ ,  $\text{Br}^-$ ,  $\text{SO}_4^{2-}$ ,  $\text{NO}_3^-$ ,  $\text{HPO}_4^{2-}$ ,  $\text{SO}_3^{2-}$ .  $\lambda_{\text{ex}} = 510 \text{ nm}$ , slit: 5 nm/5 nm.

**Mechanism of Probe 1 Responding to Cys and  $\text{SO}_2$ .** To verify whether the spectroscopic differences of **1** towards Cys and sulfite were caused by the different sensing mechanisms designed initially, we synthesized a probe-thiols adduct analogue **1-ME** and measured  $^1\text{H}$  NMR titration experiments.  $^1\text{H}$  NMR comparison data of **1** and **1-ME** in  $\text{DMSO}-d_6$  displayed that the original signals at 8.09 and 7.73 which belong to the  $\alpha,\beta$ -unsaturated ketone protons of **1** disappeared, and new signals at 4.56, 3.71 and 3.61 appeared (Figure S10). At the same time, the signal of aldehyde hydrogen still existed. Further, the fluorescent emission spectra of **1-Cys** and **1-ME** in PBS/DMSO system are similar (Figure S11). These results demonstrated that -SH induced fluorescent enhancement was caused by the nucleophilic addition reaction of sulfhydryl towards the  $\alpha,\beta$ -unsaturated ketone in **1**. Furthermore, the HR-MS data of the Cys-probe **1** system in Figure S13 also supported the same aforementioned mechanism. For  $\text{Na}_2\text{SO}_3$  detection system,  $^1\text{H}$  NMR titration experiments upon addition of  $\text{Na}_2\text{SO}_3$  to the solution of **1** in  $\text{DMSO}-d_6$  displayed that the original aldehyde hydrogen signal at 10.04 shifted to upfield at 4.99 which attributed to the addition of  $\text{SO}_3^{2-}$  to the aldehyde group of **1** (Figure S14). HR-MS data of  $\text{SO}_3^{2-}$ -probe **1** system further demonstrated the sensing mechanism (Figure S15). These results certified the predication of the probe to detect thiols and  $\text{SO}_3^{2-}$  through two reaction sites.

**Fluorescent Imaging of Thiols and  $\text{SO}_2$  in Living Cells.** Cytotoxicity experiments displayed minimal cytotoxicity of probe **1** towards A549 cells at a concentration of 50  $\mu\text{M}$  (81.4 % viability, Figure S16). The application of probe for cellular imaging was then measured using A549 cells. Figure 3a displayed that thiols scavenged A549 cells stained with **1** exhibited no fluorescent emission in both the green and orange channels. However, cells directly stained with **1** emerged apparent fluorescent emission in the green channel within 4 min (Figure 3b). Further, exogenous  $\text{SO}_3^{2-}$  in the thiols scavenged A549 cells exhibited distinct fluorescent emission in the orange channel when incubated with **1** for 4 min (Figure 3c). The above data indicated that **1** was cytolemma-permeable and could image the endogenous thiols and exogenous  $\text{SO}_3^{2-}$  through two emission channels with high selectivity in living A549 cells. Besides, the fast signal out-put further supported the probe to be used for real-time thiols imaging in cells.

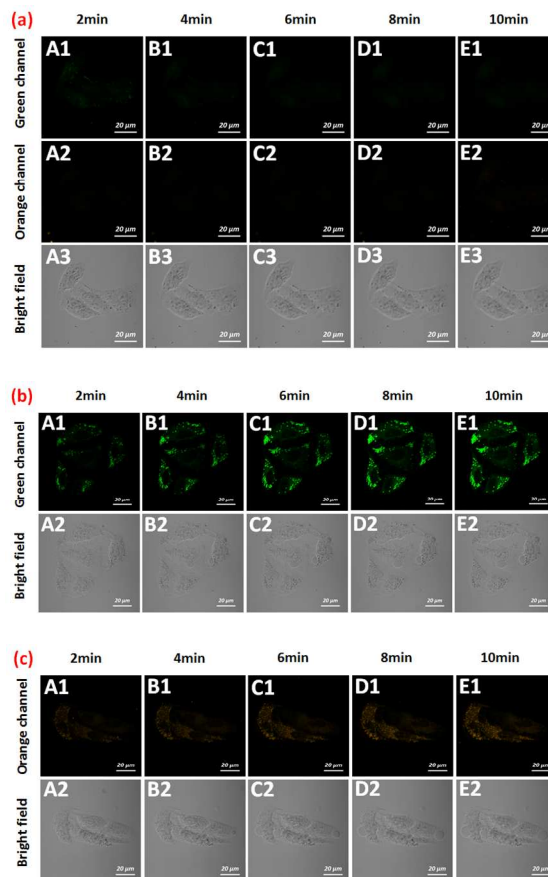


**Figure 3.** Time-dependent confocal images of endogenous thiols and exogenous  $\text{SO}_3^{2-}$  in A549 cells. a) A549 cells pre-treated with 1 mM NEM, then incubated with **1** (10  $\mu\text{M}$ ). b) A549 cells incubated with **1** (10  $\mu\text{M}$ ). c) A549 cells pre-treated with 1 mM NEM, then incubated with 200  $\mu\text{M}$   $\text{Na}_2\text{SO}_3$  for 20 min, and further incubated with **1** (10  $\mu\text{M}$ ). Green channel:  $\lambda_{\text{em}} = 490\text{-}520 \text{ nm}$  ( $\lambda_{\text{ex}} = 405 \text{ nm}$ ); Orange channel:  $\lambda_{\text{em}} = 550\text{-}590 \text{ nm}$  ( $\lambda_{\text{ex}} = 514 \text{ nm}$ ). Scale bar: 20  $\mu\text{m}$ .

**Fluorescent Imaging of Cys and  $\text{SO}_2$  in Zebrafish.** To validate the feasibility of **1** to image Cys and  $\text{SO}_3^{2-}$  in vivo, we applied **1** in living zebrafish imaging. As shown in Figure 4, NEM pre-treated 5-day-old zebrafish to load **1** display nearly no fluorescence emission in both the green and orange channels (A1-A3). However, the NEM pre-treated zebrafish further treated with Cys (B1-B3) and  $\text{SO}_3^{2-}$  (C1-C3) induced significant fluorescent emission after stained with **1** in the green and orange channels, respectively. D1-D3 displayed that **1** could visualize the distribution of thiols in living zebrafish. These results implied that **1** was tissue-permeable and could detect Cys and  $\text{SO}_3^{2-}$  through two emission channels in living bodies, respectively.

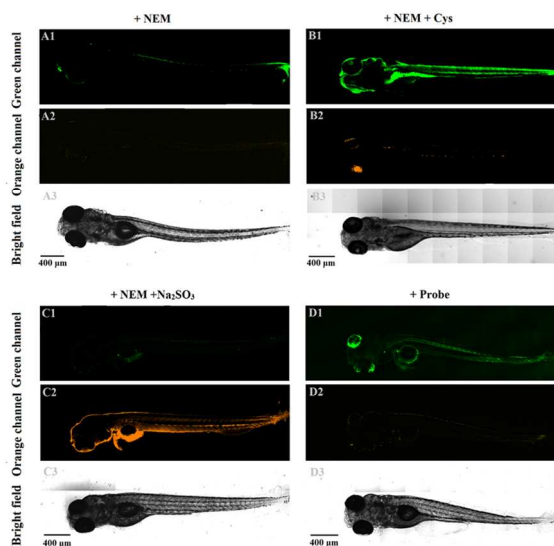


**Figure 4.** Confocal images of **1** responded to exogenous Cys and  $\text{SO}_3^{2-}$ , endogenous thiols in 5-day-old zebrafish. (A1-A3): Zebrafish was pre-treated with NEM (200  $\mu\text{M}$ ) for 15 min and then incubated with **1** (10  $\mu\text{M}$ ) for 30 min. (B1-B3), (C1-C3): Zebrafish was pre-treated with NEM (200  $\mu\text{M}$ ) for 15 min and then incubated with Cys and  $\text{Na}_2\text{SO}_3$  (100  $\mu\text{M}$ ) for 30 min, respectively, and finally incubated with **1** (10  $\mu\text{M}$ ) for 30 min. (D1-D2): Zebrafish was incubated with **1** (10  $\mu\text{M}$ ) for 30 min. From top to bottom: Green channel:  $\lambda_{\text{em}} = 490\text{-}520 \text{ nm}$  ( $\lambda_{\text{ex}} = 405 \text{ nm}$ ); Orange channel:  $\lambda_{\text{em}} = 550\text{-}590 \text{ nm}$  ( $\lambda_{\text{ex}} = 488 \text{ nm}$ ); Bright field. Scale bar: 400  $\mu\text{m}$ .

**Fluorescent Imaging of  $\text{H}_2\text{O}_2$  Induced Redox Dynamic in Living Cells.** Promoted by the  $\text{H}_2\text{O}_2$  induced reversibility of the Cys-probe **1** system in vitro, we valued the performance of **1** to monitor the redox dynamic in A549 cells stimulated by  $\text{H}_2\text{O}_2$ . Figure 5b and 5c displayed that **1** loaded A549 cells featured stable fluorescent emission in the green channel within 60 min. However,  $\text{H}_2\text{O}_2$  incubation of the **1** loaded A549 cells displayed distinct fluorescent quenching in the following 60 min, especially after 20 min incubating (Figure 5a and 5c). This result might be caused by the consumption of  $\text{H}_2\text{O}_2$  by the original existed GSH in cells in the initially 20 min, which did not cause apparent fluorescent changes. After equilibrium, **1**-Cys was reduced and the fluorescent emission was quenched. These results indicated that the probe could image thiols in A549 cells with good photostability and could be used to imaging the redox dynamic in A549 cells.

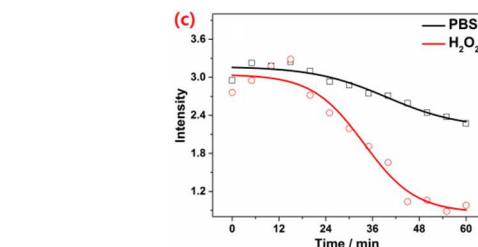
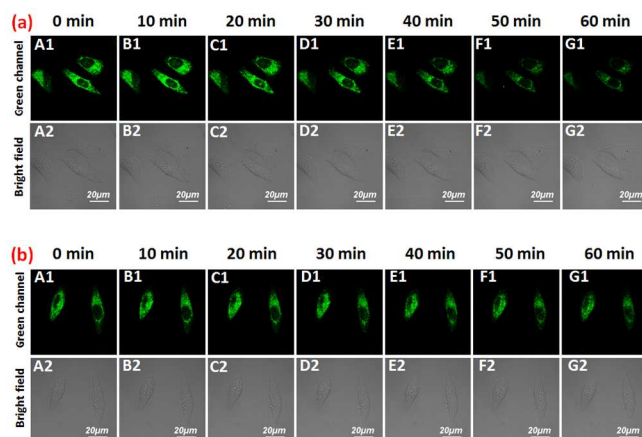


**Figure 5.** Time-dependent thiols imaging with **1** (10  $\mu\text{M}$ ) in A549 cells upon  $\text{H}_2\text{O}_2$  treatment. a) A549 cells were pre-treated with **1** (10  $\mu\text{M}$ ) for 20 min, then washed by PBS (10 mM, pH = 7.4) three times, then  $\text{H}_2\text{O}_2$  (200  $\mu\text{M}$ ) was added. b) A549 cells were treated with **1** (10  $\mu\text{M}$ ) for 20 min, then washed by PBS (10 mM, pH = 7.4) three times. Confocal images were then obtained. From top to bottom: Green channel:  $\lambda_{\text{em}} = 490\text{-}520 \text{ nm}$  ( $\lambda_{\text{ex}} = 405 \text{ nm}$ ), Bright field. Scale bar: 20  $\mu\text{m}$ . c) The corresponding time-dependent arithmetic mean intensity changes of the  $\text{H}_2\text{O}_2$  or PBS treated cell images.

### Fluorescent Imaging of Cys Metabolism in Living Cells.

Supported by the former cellular experiments, we assumed that long time imaging of Cys loaded A549 cells might monitor the metabolism of Cys. Thus, we performed time-dependent cell experiments using A549 cells. As shown in Figure 6a, after treated with 1 mM NEM, 100  $\mu\text{M}$  Cys and 10  $\mu\text{M}$  **1** successively, the strong fluorescent emission in the green channel quenched gradually in the following 240 min which reflected the consumption of Cys in cells. Correspondingly, the initial dim fluorescent emission in the orange channel increased which meant the endogeneity of  $\text{SO}_2$  (Figure 6b). The ratio images ( $R_{O/G}$ ) established by fluorescent detection of orange channel and green channel using Carestream software displayed the concentration changes of Cys and  $\text{SO}_2$ . The present experiments substantiated the Cys metabolism to produce  $\text{SO}_2$  in living A549 cells. Further, as far as we know, this was the first time for fluorescent probes to imaging the endogenous generated  $\text{SO}_2$  without incubation of the  $\text{SO}_2$  donors such as  $\text{Na}_2\text{S}_2\text{O}_3$  and 2,4-dinitrobenzene sulfonamide.

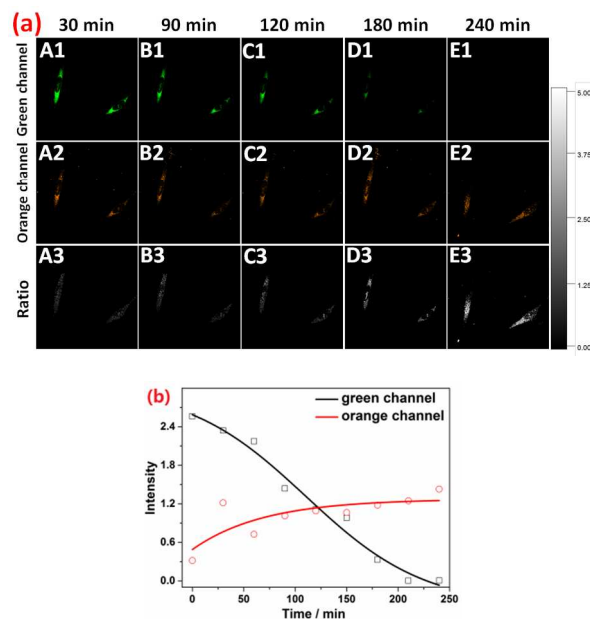


**Figure 6.** Cys metabolism imaging with **1** (10  $\mu\text{M}$ ) in A549 cells. a) A549 cells incubated with 1 mM NEM for 30 min, 100  $\mu\text{M}$  Cys

for 30 min and 10  $\mu\text{M}$  **1** for 20 min, successively. After washing with PBS, confocal images were obtained. From top to bottom: Green channel:  $\lambda_{\text{em}} = 490\text{-}520$  nm ( $\lambda_{\text{ex}} = 405$  nm), Orange channel:  $\lambda_{\text{em}} = 550\text{-}590$  nm ( $\lambda_{\text{ex}} = 488$  nm), Ratio images ( $R_{\text{O/G}}$ ). b) The corresponding time-dependent arithmetic mean intensity changes of the obtained images.

## CONCLUSION

In conclusion, we have developed the first fluorescent probe for Cys metabolism visualization based on the rational design of the dual recognition sites for Cys and its metabolite  $\text{SO}_2$ , respectively. The probe featured fast and reversible fluorescent responses towards Cys which promoted the probe to monitor the Cys concentration alterations induced by NEM and  $\text{H}_2\text{O}_2$  in vitro. Further, with high selectivity towards thiols and  $\text{SO}_2$ , the probe was successfully applied for exogenous Cys and  $\text{SO}_2$  imaging in zebrafish. Cellular experiments demonstrated that the probe could be used for redox dynamic imaging in A549 cells. Importantly, with ratiometric fluorescent responses, the probe could visualize the enzymatic conversion of Cys to  $\text{SO}_2$  in living A549 cells which provided a deeper insight into the physiological processes of Cys. Supported by the present work, fluorescent probes to image the metabolism of other important thiols are developing in our lab, and we believe that these probes will bring a better understanding to the pathological roles of biothiols.

## ASSOCIATED CONTENT

**Supporting Information.** Supplemental figures, synthetic schemes and experimental procedures, and characterization of all compounds. This material is available free of charge via the Internet at <http://pubs.acs.org>.

## AUTHOR INFORMATION

### Corresponding Author

\*M.X. Meng  
mengxm@ahu.edu.cn.

\*C.X. Yin  
yincx@sxu.edu.cn

### Author Contributions

§ Fangjun Huo and Yongkang Yue contributed equally.

### Notes

The authors declare no competing financial interests.

## ACKNOWLEDGMENT

The work was supported by the National Natural Science Foundation of China (No. 21472118, 21672131, 21372005), Talents Support Program of Shanxi Province (2014401), Shanxi Province Outstanding Youth Fund (No. 2014021002).

## REFERENCES

- (1) (a) Ubuka, T.; Ohta, J.; Yao, W. B.; Abe, T.; Teraoka, T.; Kurozumi, Y. *Amino acids* **1992**, *2* (1-2), 143-55; (b) Du, S. X.; Jin, H. F.; Bu, D. F.; Zhao, X.; Geng, B.; Tang, C. S.; Du, J. B. *Acta pharmacol. Sin.* **2008**, *29* (8), 923-30; (c) Luo, L.; Chen, S.; Jin, H.; Tang, C.; Du, J. *Biochem. Bioph. Res. Commun.* **2011**, *415* (1), 61-7; (d) Stipanuk, M. H.; Ueki, I. *J. Inherit. Metab. Dis.* **2011**, *34* (1), 17-32; (e) Xu, W.; Teoh, C. L.; Peng, J.; Su, D.; Yuan, L.; Chang, Y. T. *Biomaterials* **2015**, *56*, 1-9.
- (2) (a) Jung, H. S.; Han, J. H.; Pradhan, T.; Kim, S.; Lee, S. W.; Sessler, J. L.; Kim, T. W.; Kang, C.; Kim, J. S. *Biomaterials* **2012**, *33* (3), 945-53; (b) Jung, H. S.; Pradhan, T.; Han, J. H.; Heo, K.

J.; Lee, J. H.; Kang, C.; Kim, J. S. *Biomaterials* **2012**, *33* (33), 8495-502.

(3) (a) Lehmann, A. *Neurosci.* **1987**, *22* (2), 573-578; (b) Heafield, M. T.; Fearn, S.; Steventon, G. B.; Waring, R. H.; Williams, A. C.; Sturman, S. G. *Neurosci. Lett.* **1990**, *110* (1-2), 216-220.

(4) (a) Huo, F. J.; Sun, Y. Q.; Su, J.; Chao, J. B.; Zhi, H. J.; Yin, C. X. *Org. Lett.* **2009**, *11* (21), 4918-21; (b) Niu, L. Y.; Guan, Y. S.; Chen, Y. Z.; Wu, L. Z.; Tung, C. H.; Yang, Q. Z. *Chem. Commun.* **2013**, *49* (13), 1294-6.

(5) (a) Liu, J.; Sun, Y. Q.; Huo, Y.; Zhang, H.; Wang, L.; Zhang, P.; Song, D.; Shi, Y.; Guo, W. *J. Am. Chem. Soc.* **2014**, *136* (2), 574-577; (b) Liu, Y.; Yu, D.; Ding, S.; Xiao, Q.; Guo, J.; Feng, G. *ACS Appl. Mater. Inter.* **2014**, *6* (20), 17543-50; (c) Yang, X. F.; Huang, Q.; Zhong, Y.; Li, Z.; Li, H.; Lowry, M.; Escobedo, J. O.; Strongin, R. M. *Chem. Sci.* **2014**, *5* (6), 2177-2183; (d) Liu, Y.; Lv, X.; Hou, M.; Shi, Y.; Guo, W. *Anal. Chem.* **2015**, *87* (22), 11475-83; (e) Chen, H.; Tang, Y.; Ren, M.; Lin, W. *Chem. Sci.* **2016**, *7* (3), 1896-1903; (f) Gong, D.; Tian, Y.; Yang, C.; Iqbal, A.; Wang, Z.; Liu, W.; Qin, W.; Zhu, X.; Guo, H. *Biosens. Bioelectron.* **2016**, *85*, 178-83; (g) Kim, C. Y.; Kang, H. J.; Chung, S. J.; Kim, H. K.; Na, S. Y.; Kim, H. J. *Anal. Chem.* **2016**, *88* (14), 7178-82; (h) Zhang, H.; Liu, R.; Liu, J.; Li, L.; Wang, P.; Yao, S. Q.; Xu, Z.; Sun, H. *Chem. Sci.* **2016**, *7* (1), 256-260.

(6) Umezawa, K.; Yoshida, M.; Kamiya, M.; Yamasoba, T.; Urano, Y. *Nat. Chem.* **2016**, 10.1038/nchem.2648.

(7) (a) Jiang, X.; Yu, Y.; Chen, J.; Zhao, M.; Chen, H.; Song, X.; Matzuk, A. J.; Carroll, S. L.; Tan, X.; Sizovs, A.; Cheng, N.; Wang, M. C.; Wang, J. *ACS Chem. Biol.* **2015**, *10* (3), 864-74; (b) Chen, J.; Jiang, X.; Carroll, S. L.; Huang, J.; Wang, J. *Org. Lett.* **2015**, *17* (24), 5978-81.

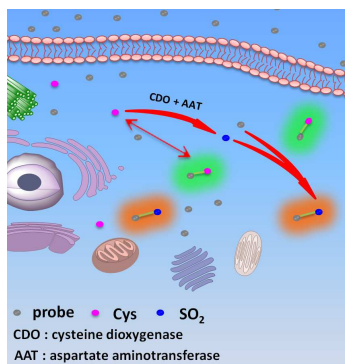
(8) (a) Yue, Y. K.; Huo, F. J.; Li, X. Q.; Wen, Y.; Yi, T.; Salamanca, J.; Escobedo, J. O.; Strongin, R. M.; Yin, C. X. *Org. Lett.* **2017**, *19*, 82-85; (b) Yang, J.; Li, K.; Hou, J. T.; Li, L.-L.; Lu, C. Y.; Xie, Y. M.; Wang, X.; Yu, X. Q. *ACS Sensors* **2016**, *1* (2), 166-172; (c) Chen, W.; Fang, Q.; Yang, D.; Zhang, H.; Song, X.; Foley, J. *Anal. Chem.* **2015**, *87* (1), 609-16; (d) Wu, M. Y.; Li, K.; Li, C. Y.; Hou, J. T.; Yu, X. Q. *Chem. Commun.* **2014**, *50* (2), 183-5; (e) Sun, Y. Q.; Liu, J.; Zhang, J.; Yang, T.; Guo, W. *Chem. Commun.* **2013**, *49* (26), 2637-9; (f) Cheng, X.; Jia, H.; Feng, J.; Qin, J.; Li, Z. *J. Mater. Chem. B* **2013**, *1* (33), 4110-4.

(9) (a) Yu, S.; Yang, X.; Shao, Z.; Feng, Y.; Xi, X.; Shao, R.; Guo, Q.; Meng, X. *Sensor. Actuat. B: Chem.* **2016**, *235*, 362-369; (b) Yang, X.-F.; Zhao, M.; Wang, G. *Sensor. Actuat. B: Chem.* **2011**, *152* (1), 8-13; (c) Xie, H.; Zeng, F.; Yu, C.; Wu, S. *Polym. Chem.* **2013**, *4* (21), 5416-5424.

(10) (a) Zhang, Y.; Guan, L.; Yu, H.; Yan, Y.; Du, L.; Liu, Y.; Sun, M.; Huang, D.; Wang, S. *Anal. Chem.* **2016**, *88* (8), 4426-31; (b) Yang, X.; Zhou, Y.; Zhang, X.; Yang, S.; Chen, Y.; Guo, J.; Li, X.; Qing, Z.; Yang, R. *Chem. Commun.* **2016**, *52* (67), 10289-92.

(11) (a) Zhang, Y.; Shao, X.; Wang, Y.; Pan, F.; Kang, R.; Peng, F.; Huang, Z.; Zhang, W.; Zhao, W. *Chem. Commun.* **2015**, *51* (20), 4245-8; (b) Lee, H. Y.; Choi, Y. P.; Kim, S.; Yoon, T.; Guo, Z.; Lee, S.; Swamy, K. M.; Kim, G.; Lee, J. Y.; Shin, I.; Yoon, J. *Chem. Commun.* **2014**, *50* (53), 6967-9; (c) Hong, R.; Han, G.; Fernandez, J. M.; Kim, B. J.; Forbes, N. S.; Rotello, V. M. *J. Am. Chem. Soc.* **2006**, *128* (4), 1078-9.

(12) (a) Hill, J. W.; Coy, R. B.; Lewandowski, P. E. *J. Chem. Edu.* **1990**, *67* (2), 172; (b) Rhee, S. G.; Bae, Y. S.; Lee, S. R.; Kwon, J. *Science's STKE* **2000**, *2000* (53), pe1; (c) Luo, D.; Smith, S. W.; Anderson, B. D. *J. Pharm. Sci.* **2005**, *94* (2), 304-16; (d) Gough, D. R.; Cotter, T. G. *Cell Death Dis.* **2011**, *2*, e213; (e) Garcia-Santamarina, S.; Boronat, S.; Hidalgo, E. *Biochemistry* **2014**, *53* (16), 2560-80.



1  
2  
3  
4  
5  
6  
7  
8  
9  
10  
11  
12  
13  
14  
15  
16  
17  
18  
19  
20  
21  
22  
23  
24  
25  
26  
27  
28  
29  
30  
31  
32  
33  
34  
35  
36  
37  
38  
39  
40  
41  
42  
43  
44  
45  
46  
47  
48  
49  
50  
51  
52  
53  
54  
55  
56  
57  
58  
59  
60